

Analytical model for structured light propagation through a turbulent atmosphere

Konstantin Kravtsov*

Technology Innovation Institute, Abu Dhabi, UAE

(Dated: May 29, 2026)

We develop a straightforward analytical framework for the propagation of spatial light modes through a turbulent atmosphere. Built upon the split-step approach with the mode-based optical field representation, it directly assesses how turbulence-induced phase fluctuations deplete the optical power in the original mode and re-distribute it into neighboring spatial modes. Importantly, this power transfer scales linearly with the propagation distance in a uniform channel, yielding a simple solution for arbitrary distances in the form of a matrix exponential. The transfer rate is determined by the spatial spectral overlap between the turbulence spectrum and the acceptance spectrum for a pair of interacting spatial modes. The model predicts the average power in each spatial mode and is exact when a single mode strongly dominates all others. Our predictions show reasonably good agreement with simulations up to medium-to-strong turbulence levels. The model also confirms the scalings with mode order previously known as empirical observations.

I. INTRODUCTION

Free-space optical communications are becoming increasingly important in today's economy. Especially with the development of *quantum* communications, there is a growing demand for the transmission of high-dimensional quantum states [1, 2]. The spatial degree of freedom, i.e., spatial *structuring* of light, is a perfect resource for both high-dimensional state transmission [3] and channel multiplexing [4].

Nevertheless, the value of this resource may be limited by unavoidable imperfections in the atmospheric channel, which arise from turbulent processes in the air. They cause spatial mode cross-talk and loss of signal in a particular mode.

Communications with structured light in atmospheric channels were extensively studied in a large number of publications, including those focusing on orbital angular momentum (OAM) modes [5–8]. The degradation of spatial quantum states in such channels was also investigated both experimentally [9] and in simulations [10, 11]. The performance of different types of spatial modes was analyzed in order to optimize the properties of the channel [12]. References to many more related studies can be found in review papers [13, 14].

Despite being well developed, this field has historically been centered on empirical observations and the extensive use of simulation tools, from early examples [15, 16] to more recent ones [14, 17, 18]. To our knowledge, if we exclude publications that either rely on explicit random phase-screen generation or employ the quadratic approximation to the Kolmogorov structure function, the only analytical model that describes the performance of a single spatial mode in a turbulent environment is our previous work [19]. It focused on the lowest order term in a series expansion of a turbulent perturbation that helped

to obtain analytical expressions for channel properties.

The present work is an accurate analytical study of the same problem that leads to exact results for a broad range of cases. In particular, it studies free-space optical channels excited at the input with a single spatial mode. Propagation in the turbulent medium causes modal cross-talk, so the optical power leaks from the original mode into other available ones. The model provides the expected average power distribution among the modes.

In the present study, we focus only on *scalar* spatial modes. The same may be applied to *vector* modes in a straightforward way, as the latter are superpositions of the former in two non-interacting polarization domains [20]. Our results for Gaussian modes with two different types of symmetry could also be adapted to other types of spatial modes. However, the general trends of mode propagation in turbulent environments are the same for arbitrary mode types, cf. [21].

The paper is organized as follows. Section II reviews key results on atmospheric turbulence and light propagation. In Section III we define our framework and provide the main results. Section IV specifically discusses propagation of a Gaussian beam as a representative example. In Section V we analyze the applicability of the model and its specific details.

II. SELECTED RESULTS ON LIGHT PROPAGATION IN TURBULENCE

Turbulent distortions of light propagating through a turbulent medium originate from tiny refraction index fluctuations around its mean value. The major result derived by Kolmogorov and confirmed by many experimental studies is that the structure function of the refraction index n in a uniform and isotropic turbulent atmosphere (in 3 dimensions) scales with the distance r as $r^{2/3}$ [22]:

$$D_n(r) \equiv \left\langle (n(r) - n(0))^2 \right\rangle = C_n^2 r^{2/3}, \quad (1)$$

* konstantin.kravtsov@tii.ae

where C_n^2 is the so-called refractive index structure constant. Switching to the Fourier domain, defined by the corresponding wavenumbers K , the previous expression is equivalent to the spatial power spectrum $\Phi_n(K)$ in the form

$$\Phi_n(K) = \frac{5}{18\pi\Gamma(1/3)} C_n^2 K^{-11/3} \approx 0.033 C_n^2 K^{-11/3}, \quad (2)$$

where $\Gamma(x)$ is the gamma function. Strictly speaking, the given scaling is observed only for some range of distances r (and, correspondingly, wavenumbers K in the Fourier domain) between the inner (l_0) and the outer (L_0) scales of turbulence [23], where $l_0 < L_0$. However, we will ignore it for now.

The next important result is a transition from refractive index perturbations to fluctuations of optical phase S for a paraxial optical beam with wavelength λ and wavenumber $k = 2\pi/\lambda$ after the propagated distance of L . The derivation of the optical phase structure function $D_S(\rho)$ and its power spectrum $F_S(K)$ in a 2-dimensional plane perpendicular to the light propagation direction yields [22]

$$D_S(\rho) \equiv \left\langle (S(\rho) - S(0))^2 \right\rangle = 4\pi \int_0^\infty K [1 - J_0(K\rho)] F_S(K) dK, \quad (3)$$

where J_0 is the Bessel function of the first kind, and the 2-D transverse distance ρ is explicitly used instead of the 3-D distance r to avoid ambiguity. Notably, the 2-D phase fluctuation spectrum coincides with the 3-D spectrum of the refractive index fluctuations up to a constant:

$$F_S(K) = 2\pi k^2 L \Phi_n(K) \approx 0.207 C_n^2 k^2 L K^{-11/3} \quad (4)$$

The evaluation of the integral (3) yields

$$D_S(\rho) = 2 \frac{\sqrt{\pi} \Gamma(1/6)}{5\Gamma(2/3)} C_n^2 k^2 L \rho^{5/3} \approx 2 \times 1.46 C_n^2 k^2 L \rho^{5/3}. \quad (5)$$

Another conventional form of the expression for the phase structure function was proposed by Fried [24]

$$D_S(\rho) = 8\sqrt{2} \left[\frac{3}{5} \Gamma\left(\frac{6}{5}\right) \right]^{5/6} \left(\frac{\rho}{r_0} \right)^{5/3} \approx 6.88 \left(\frac{\rho}{r_0} \right)^{5/3}, \quad (6)$$

where r_0 is the Fried parameter. In a sense, r_0 defines the best angular resolution achievable when observing through a turbulent channel: it corresponds to the diffraction-limited resolution of a telescope with an aperture diameter equal to r_0 [25]. Comparing the last two expressions gives a definition of the Fried parameter

$$r_0 = (0.42 C_n^2 k^2 L)^{-3/5}. \quad (7)$$

Looking at given expressions for structure functions (or spectra), we can see that they diverge as $\rho \rightarrow \infty$ (or $K \rightarrow$

0). Formally, this means that at an arbitrary point in the transverse plane, the phase variance given by the integral $(2\pi)^{-2} \iint_0^\infty F_S(K) dK_x dK_y$ is infinite, since the integral diverges as $K \rightarrow 0$. In fact, this is the reason why a more complex description based on the structure function is chosen instead of a more conventional covariance-based approach. This divergence is unphysical and stems from the continuation of (1) beyond the applicable range of arguments from l_0 to L_0 .

The problem is resolved by attenuating the spectrum of fluctuations outside this range. One common way to do this is to express the spectrum Φ_n or F_S via the spatial frequency $f = K/(2\pi)$ and substitute

$$f^{-11/3} \rightarrow \frac{\exp(-l_0^2 f^2)}{(f^2 + L_0^{-2})^{11/6}}, \quad (8)$$

which corresponds to the so-called modified von Karman turbulence model [22].

Finally, another important quantity that will appear in the present paper defines the strength of turbulence for a given optical channel and is called the Rytov parameter σ_R^2 . It is defined as the variance of $\ln(I/I_0)$ for low turbulence levels, where I is the intensity observed at a given point in the output plane of the channel, assuming that the input plane contains an ideal plane wave; and I_0 is an arbitrary reference intensity. As derived in [26] for the spectrum (2)

$$\sigma_R^2 = 4 \frac{2^{1/6} \pi^{3/2} (\sqrt{3} - 1)}{11 \Gamma(2/3)} C_n^2 k^{7/6} L^{11/6} \approx 1.23 C_n^2 k^{7/6} L^{11/6}. \quad (9)$$

For larger $\sigma_R^2 \gtrsim 0.5$ its connection with log-intensity fluctuations breaks, as the experimentally measured fluctuations tend to saturate around $\sigma_{\ln I}^2 \approx 1$ [22, 23].

III. MODAL ANALYSIS FRAMEWORK

We study the propagation of spatial modes of light in a turbulent medium, as schematically depicted in Fig. 1a. Following the conventional split-step representation of the channel, we can divide it into a large number of infinitesimal pieces as shown in Fig. 1b. Each of them can be treated as a localized phase perturbation and a corresponding free propagation region. The key element of the proposed approach is focusing on discrete spatial optical modes rather than on the entire electromagnetic field distribution. The modes themselves are eigenfunction solutions of the propagation equation and allow one to avoid dealing with the propagation equation of the electromagnetic field per se. In particular, we only account for the optical power in each of the modes as shown graphically at the input and output of the channel.

An apparent advantage of such an encoding is its invariance under free propagation. Thus, one of the two components in the split-step model disappears, while only the accumulated effects of infinitesimal phase

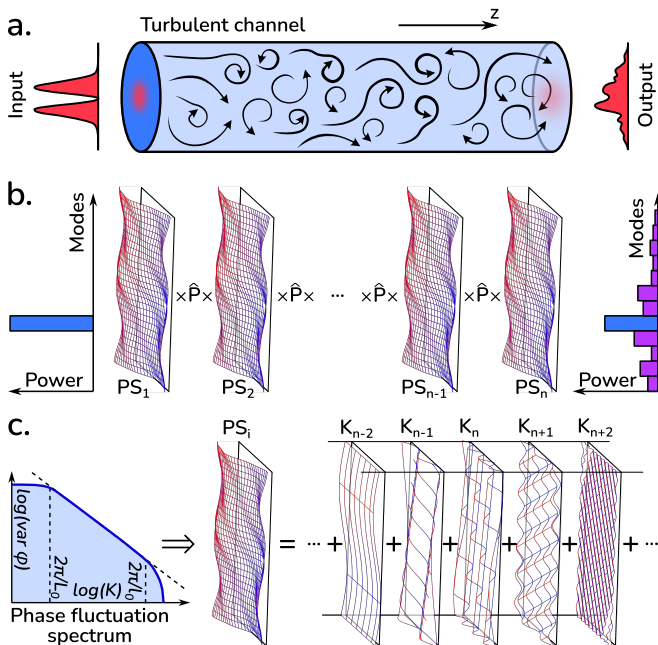


FIG. 1. Key elements of the proposed framework.

a. Schematic of the implied physical setup: a single spatial mode of light enters an extended channel with a turbulent medium, where it gets distorted. **b.** The same problem in the split-step representation: the channel is divided into a large number of random and independent chunks. Each chunk is modeled as a zero-thickness phase screen (PS_i) and a free propagation region defined by the propagator \hat{P} . The resulting field in the end of the channel is decomposed into spatial modes to analyze their statistics. Our key proposal is to use the depicted *optical-power-versus-spatial-mode* encoding, which turns \hat{P} into the identity operator; therefore, the overall effect of the channel is just a collective action of infinitesimal phase screens. **c.** Each phase screen is defined by a given spatial spectrum of phase fluctuations (left). It allows each infinitesimal phase screen to be represented as a sum of a large number of elementary phase waves with random directions and varying wavevectors K_i .

screens on the modal distribution remain. This greatly simplifies the problem and makes it analytically integrable, as we show below. At the same time, this encoding ignores the relative phases between spatial modes, which has consequences for the applicability of the model discussed in depth in Section V.

Each infinitesimal phase screen follows the same shape of the spatial power spectrum (see Fig. 1c.) and can be perceived as a large set of independent phase perturbations of different spatial frequencies. Therefore, we model the resulting effect of a phase screen as a direct sum of elementary harmonic phase distortions (waves) with certain spatial frequencies and amplitudes. Their directions in the plane perpendicular to the light propagation direction and absolute phases are random. Each individual perturbation is weak and independent of the others.

The induced phase fluctuations associated with each infinitesimal phase screen break the orthogonality between spatial modes and lead to power redistribution among the modes. First, we study this effect for an elementary single-frequency phase wave contributing to an extremely weak phase screen. Second, we combine contributions for the entire ensemble of those elementary waves with varying spatial frequency to arrive at the contribution of an individual phase screen. Finally, an extended channel is constructed from the infinite number of individual phase screen contributions.

We adopt the following notation: z is the direction of the paraxial beam propagation; x and y define the perpendicular plane. All modes are centered on $x = y = 0$. We also use the cylindrical coordinate system ρ, θ, z .

We explicitly study two convenient mode sets: Hermite-Gaussian (HG) and Laguerre-Gaussian (LG), however any other orthogonal mode set can be used similarly. $G(x, y)$ (or $G(\rho, \theta)$) is the mode field profile in the transverse plane; the indices a and b fully specify the corresponding modes.

The orthogonality of the mode set indicates that

$$\iint_{-\infty}^{\infty} G_a(x, y) G_b^*(x, y) dx dy = \delta_{ab}, \quad (10)$$

i.e., zero if $a \neq b$; where $*$ denotes the complex conjugation. The onset of a phase wave with the wavenumber $K = \sqrt{K_x^2 + K_y^2}$ and the amplitude α_K

$$\varphi_K(x, y) = \alpha_K \cos(K_x x + K_y y + \phi) \quad (11)$$

breaks this orthogonality. So, the fraction of power that migrates from mode a to mode b due to the perturbation (cf. the transition probability) is the squared modulus of the transition amplitude

$$P_{ab}(K) = |A_{ab}(K)|^2 = \left| \iint_{-\infty}^{\infty} G_a(x, y) G_b^*(x, y) \exp[i\varphi_K(x, y)] dx dy \right|^2. \quad (12)$$

One can see that $P_{ab}(K)$ is independent of the mode ordering. In addition, if the particular mode set is complete, power conservation requires that $\sum_b P_{ab}(K) = 1$.

Since each elementary single-frequency phase wave is a tiny contribution to the infinitesimal phase screen, we use the following power series decomposition ignoring higher order terms

$$\exp[i\varphi(x, y)] = 1 + i\varphi(x, y) - \varphi^2(x, y)/2 + O(\varphi^3). \quad (13)$$

Hermite-Gaussian modes may be described by the following expression that ignores the global phase that is independent of the transverse coordinates

$$HG_{mn}(x, y) = \sqrt{\frac{kz_R}{\pi}} \frac{\exp\left[-k(x^2 + y^2)/2(z_R - iz)\right]}{\sqrt{2^{m+n} n! m! (z_R - iz)}} \times H_m\left(x\sqrt{\frac{kz_R}{z_R^2 + z^2}}\right) H_n\left(y\sqrt{\frac{kz_R}{z_R^2 + z^2}}\right), \quad (14)$$

where $z_R = \pi w_0^2/\lambda$ is the Rayleigh length, H_n is the Hermitian polynomial of order n , $i^2 = -1$, and $z = 0$ defines the position of the beam waist. Each mode is defined by a pair of non-negative integer indices m and n , while their sum is designated as N and defines the mode order $N = m + n$.

Laguerre-Gaussian modes have cylindrical symmetry and thus are defined in the cylindrical coordinates instead. Their transverse profile is given by

$$LG_{pl}(\rho, \theta) = \sqrt{\frac{p!}{\pi(p+|l|)!}} \left(\frac{\sqrt{kz_R}}{z_R - iz} \right)^{|l|+1} \rho^{|l|} e^{il\theta} \times L_p^{|l|} \left(\frac{kz_R \rho^2}{z_R^2 + z^2} \right) \exp \left[-\frac{k\rho^2}{2(z_R - iz)} \right], \quad (15)$$

where L_q^s is the generalized Laguerre polynomial. The mode is defined by a non-negative integer p and an integer l . The mode order for LG modes is $N = 2p + |l|$.

Each mode in one of the sets is a linear combination of modes of the same order N in the other set [27, 28]. Both mode sets have a distance-varying spot radius

$$w(z) = w_0 \sqrt{1 + (z/z_R)^2}. \quad (16)$$

So, the parameter w_0 has the meaning of the characteristic waist radius, while z_R is one half of the waist length. In order to provide a dimensionless representation of the involved calculus, we will extensively use the following dimensionless variable

$$\vartheta_K = K^2 \frac{z_R^2 + z^2}{4kz_R} = \frac{K^2 w^2(z)}{8}, \quad (17)$$

which is roughly the number of full phase waves per mode diameter squared. To simplify the notation, we will often omit the subscript for ϑ and the argument for w below.

A. Interaction of Laguerre-Gaussian modes

The analog of (12) for LG modes in cylindrical coordinates is

$$A_{pl:qs}^{LG} = \int_0^\infty \rho d\rho \int_0^{2\pi} d\theta LG_{pl}(\rho, \theta) LG_{qs}^*(\rho, \theta) \exp[i\varphi(\rho, \theta)]. \quad (18)$$

Due to cylindrical symmetry, this quantity does not depend on the direction (K_x, K_y) of the phase wave, so without loss of generality we may assume $K_x = K$, $K_y = 0$, and the argument of the cos function in (11) becomes $K\rho \cos \theta + \phi$.

We evaluate integrals in (18) using (cf. [29, 8.411.2-3])

$$\int_0^{2\pi} e^{i(l-s)\theta} \cos(\kappa r \cos \theta + \phi) d\theta = \pm 2\pi J_{|l-s|}(\kappa r) \begin{cases} \cos \phi & \text{if } l-s \text{ is even,} \\ \sin \phi & \text{otherwise,} \end{cases} \quad (19)$$

where J_n is the Bessel function of the n -th order. Then applying [29, 7.422.2, to be corrected in future editions]

$$\int_0^\infty x^{\nu+\sigma+1} e^{-x^2} L_m^\nu(x^2) L_n^\sigma(x^2) J_{\nu+\sigma}(2yx) dx = \frac{(-1)^{m+n}}{2} y^{\nu+\sigma} e^{-y^2} L_n^{m-n+\nu}(y^2) L_m^{n-m+\sigma}(y^2), \quad (20)$$

and [29, 7.422.3, to be included in future editions]

$$\int_0^\infty x^{\nu+\sigma+1} e^{-x^2} L_m^\nu(x^2) L_n^\sigma(x^2) J_{\nu-\sigma}(2yx) dx = (-1)^{m+n} \frac{(n+\sigma)!}{2n!} y^{\nu-\sigma} e^{-y^2} L_{n+\sigma}^{m-n+\nu-\sigma}(y^2) L_m^{n-m}(y^2) \quad (21)$$

we arrive at a closed form expression. Finally, when calculating $P_{pl:qs}(K)$ we average the result over all possible phases ϕ of the phase wave, so $\langle \cos^2 \phi \rangle = \langle \sin^2 \phi \rangle = 1/2$.

The evaluation of such overlaps between different spatial modes ($p \neq q$ or $l \neq s$) is the most straightforward, since only the linear term in (13) provides the dominant contribution. So, the resulting coupling is

$$P_{pl:qs}^{LG}(K) = \frac{\alpha_K^2}{2} \frac{q!}{(q+|s|)!} \vartheta_K^{|s|} \exp(-2\vartheta_K) \times \begin{cases} \left[\frac{(p+|l|)!}{p!} \vartheta_K^{-|l|} \left[L_{p+|l|}^{q-p+|s|-|l|}(\vartheta_K) L_q^{p-q}(\vartheta_K) \right]^2 & \text{if } ls \geq 0, \\ \left[\frac{p!}{(p+|l|)!} \vartheta_K^{|l|} \left[L_p^{q-p+|s|}(\vartheta_K) L_q^{p-q+|l|}(\vartheta_K) \right]^2 & \text{if } ls \leq 0. \end{cases} \quad (22)$$

Both expressions actually coincide if $ls = 0$, which is a non-trivial fact in the case $l \neq 0$.

In the case of the same mode we have to deal with both the constant and the linear term, with the resulting expression

$$P_{pl:pl}^{LG}(K) = 1 - \frac{\alpha_K^2}{2} \left(1 - [L_{p+|l|}(\vartheta_K) L_p(\vartheta_K)]^2 \exp(-2\vartheta_K) \right) \quad (23)$$

B. Interaction of Hermite-Gaussian modes

The evaluation of (12) for the HG modes proceeds in a similar way. However, owing to the lack of rotation symmetry, the result depends on the direction of the phase wave. In the following, we use this form: $K_x = K \cos \xi$ and $K_y = K \sin \xi$.

An essential evaluation [29, 7.374.7]

$$\int_{-\infty}^\infty e^{-(x-y)^2} H_m(x) H_n(x) dx = 2^n \sqrt{\pi} m! y^{n-m} L_m^{n-m}(-2y^2), \quad (24)$$

which is valid for any positive integers $m \leq n$, is used for both x and y directions. As the final result is symmetric

with respect to the exchange $m \leftrightarrow k$ or $n \leftrightarrow t$, below we use the assumption that $m \leq k$ and $n \leq t$ for certainty. We also perform averaging over phase ϕ in the same way as for LG modes.

The result for a pair of distinct modes is as follows

$$P_{mn;kt}^{HG}(K) = \frac{\alpha_K^2}{2} \frac{m! n!}{k! t!} (2\vartheta_K \cos^2 \xi)^{k-m} (2\vartheta_K \sin^2 \xi)^{t-n} \times \left[L_m^{k-m}(2\vartheta_K \cos^2 \xi) L_n^{t-n}(2\vartheta_K \sin^2 \xi) \right]^2 \exp(-2\vartheta_K). \quad (25)$$

In the case of the same mode, the remaining power in the particular Hermite-Gaussian mode is given by

$$P_{mn;mn}^{HG}(K) = 1 - \frac{\alpha_K^2}{2} \times \left[1 - \left(L_m(2\vartheta_K \cos^2 \xi) L_n(2\vartheta_K \sin^2 \xi) \right)^2 \exp(-2\vartheta_K) \right]. \quad (26)$$

Finding these quantities for the isotropic case of real turbulence requires averaging over all possible angles $\xi \in [0, 2\pi)$. At the time of writing, an analytical approach proved infeasible (see also Section VC for analytical scalings). For practical applications, numerical averaging should be used instead.

C. Contribution of a single phase screen

So far we have calculated the interaction of spatial modes induced by an elementary phase wave of a certain wavenumber K and the infinitesimal amplitude α_K . The next step is to combine such elementary perturbations with different wavenumbers as in the actual phase screen produced by a thin layer of the turbulent atmosphere. The key condition is that, in the actual turbulent process, contributions at different wavenumbers are mutually independent. Therefore, the phase and direction of each elementary contribution are totally random, matching the assumptions we made in our calculations earlier.

By performing direct integration, we have shown that the first nonvanishing term of perturbation in the mode-coupling expressions is quadratic in the amplitude of elementary phase wave, regardless of the chosen mode family. Specifically, the integration results have the form of

$$P_{ab}(K) = \begin{cases} \alpha_K^2/2 B_{ab}(\vartheta_K), & \text{if } a \neq b, \\ 1 + \alpha_K^2/2 B_{ab}(\vartheta_K), & \text{if } a = b, \end{cases} \quad (27)$$

where $B(\vartheta_K)$ is given by different expressions for the two studied sets of modes. The diagonal elements B_{aa} are negative, as each elementary wave depletes the power in mode a , while the off-diagonal ones are positive, as a tiny part of the optical power in mode a is transferred to mode b . The key insight is that the pre-factor in each of

the expressions for the elementary perturbation, $\alpha_K^2/2$, is, in fact, the variance of the phase deviation for an elementary wave (11). However, phase variance is the additive quantity that defines the power spectrum. Indeed, for two distinct K and K' due to their independence, $\langle (\varphi_K + \varphi_{K'})^2 \rangle = \langle \varphi_K^2 \rangle + \langle \varphi_{K'}^2 \rangle$, so the contributions for different wavevectors are additive.

The combined average effect produced by an ensemble of elementary phase waves with varying K is therefore obtained as the sum of their individual contributions. At the same time, the phase variance associated with a small spectral width ΔK around the value K is defined by the 2-dimensional power spectrum $F_S(K)$ as $F_S(K) 2\pi K \Delta K$. Thus, the overall combined perturbation caused by a weak phase screen is given by

$$\int_0^\infty F_S(K) B_{ab}(\vartheta_K) 2\pi K dK. \quad (28)$$

Another insight is that $|B(\vartheta_K)| \leq 1$, that is, it may be perceived as a spectral filter that partially accepts phase perturbation power into the coupling strength between modes. So, the overall mode coupling produced by a weak phase screen is equal to the total power of its phase fluctuations attenuated by the mode-specific spectral filter $B_{ab}(\vartheta_K)$.

D. General extended turbulent channel

In an extended channel, the power of phase perturbations is also an additive quantity: each chunk of the optical path adds a certain power to phase perturbations. This follows from the linear dependence of the power spectrum $F_S(K)$ on the channel length L in (4). Therefore, the coupling rate is defined by the accumulation rate of phase fluctuations, i.e. the derivative $dF_S(K, L)/dL$. Another simplification is to use dimensionless ϑ_K instead of K as the argument of the phase perturbation spectrum. Combining these two ideas, we define the following quantity:

$$\Lambda_{ab} \equiv \int_0^\infty \frac{dF_S(K, L)}{dL} B_{ab}(\vartheta_K) 2\pi K dK = \frac{8\pi}{w^2} \int_0^\infty \frac{dF_S(\vartheta, L)}{dL} B_{ab}(\vartheta) d\vartheta. \quad (29)$$

Thus, a weak phase screen associated with a small chunk of the channel having length ΔL produces the following mode coupling:

$$P_{ab} = \begin{cases} \Lambda_{ab} \Delta L, & \text{if } a \neq b, \\ 1 + \Lambda_{ab} \Delta L, & \text{if } a = b, \end{cases} \quad (30)$$

Apparently, Λ_{ab} define a matrix, and the result for a uniform extended channel is $\mathbf{v} \approx (\mathbb{I} + \mathbf{\Lambda}L)\mathbf{v}_0$, where \mathbb{I} is the identity matrix, while \mathbf{v}_0 and \mathbf{v} are the vectors of optical powers before and after the channel in all considered

modes. This expression only works for small perturbations, as it ignores the incremental depletion of power in the excited modes and the population of the empty ones.

The accurate solution for an arbitrary channel length L is given by the matrix exponent

$$\mathbf{v} = \exp(\mathbf{\Lambda}L) \mathbf{v}_0, \quad (31)$$

which is the final result of the present study. This expression has its own limits of applicability, which are discussed in Section V.

E. Explicit results for the modified von Karman turbulence spectrum (8)

Using $K^{-11/3} = w^{11/3} \vartheta^{-11/6} / (32\sqrt{2})$ and substituting (4) into (29) with the von Karman spectral damping, one can show that in a uniform atmospheric channel

$$\begin{aligned} \Lambda_{ab} &= 0.115 C_n^2 k^2 w^{5/3} \\ &\times \int_0^\infty \left(\vartheta + \frac{\pi^2 w^2}{2L_0^2} \right)^{-11/6} \\ &\times \exp\left(-2\vartheta l_0^2 / (\pi^2 w^2)\right) B_{ab}(\vartheta) d\vartheta. \end{aligned} \quad (32)$$

Alternatively, expressing the strength of the turbulence in the form of the Fried parameter, one can find that

$$\Lambda_{ab} L = 0.272 \left(\frac{w}{r_0} \right)^{5/3} \mathcal{I}_{ab}, \quad (33)$$

where \mathcal{I}_{ab} is the same dimensionless integral over the entire spectrum that appears in (32).

In a non-uniform channel where either the strength of the turbulence or the mode width w varies with propagation, another integration should be performed over the length of the channel.

IV. POWER DEPLETION IN THE FUNDAMENTAL MODE

An important practical topic is the propagation of a Gaussian beam through the turbulent atmosphere. It can be analyzed in detail within the developed framework by looking at interactions of 00 mode with higher order ones. As discussed earlier, each chunk of the propagation distance contributes a share of phase fluctuation power that leads to re-distribution of a fraction of the optical power from the fundamental mode into higher order modes.

For LG modes using $[L_q^{-q}(\vartheta)]^2 = \vartheta^{2q} / (q!)^2$ it is convenient to re-write the acceptance spectrum for a group of modes with mode order N as

$$B_{00; \min(j, N-j), N-2j}^{LG}(\vartheta) = \frac{\vartheta^N \exp(-2\vartheta)}{j!(N-j)!}, \quad (34)$$

where integer $j \in \{0, 1, \dots, N\}$ indexes all modes in the group. Thus, the generation rates for LG modes of a given order N are proportional to the N th row of Pascal's triangle: the maximal rates are observed for central modes with minimal (or zero) OAM; in contrast, the smallest rates correspond to the modes with the highest azimuthal index.

For the HG family, we also consider a group of modes of order $N = m + n$. First, we can perform directional averaging using

$$\langle \cos^{2m} \xi \sin^{2n} \xi \rangle = \frac{(2m)! (2n)!}{4^{m+n} (m+n)! m! n!}. \quad (35)$$

Then, the resulting acceptance spectrum becomes

$$B_{00; mn}^{HG}(\vartheta) = \frac{\vartheta^N \exp(-2\vartheta)}{2^N N!} \binom{2m}{m} \binom{2n}{n}. \quad (36)$$

This distribution within the group is much more uniform than for LG modes, with some advantage for the generation of highly asymmetric modes where m or n approach N .

The acceptance spectrum for the power remaining in the fundamental mode (which is the same in both mode families) is negative and equals

$$B_{00,00}(\vartheta) = \exp(-2\vartheta) - 1. \quad (37)$$

It is straightforward to show that the combined power loss towards the group of modes of a certain order $N > 0$ is

$$B_{00,N}(\vartheta) = \frac{(2\vartheta)^N}{N!} \exp(-2\vartheta) \quad (38)$$

regardless of the chosen mode type. This result for HG modes may be obtained using

$$\sum_{k=0}^n \binom{2k}{k} \binom{2n-2k}{n-k} = 4^n. \quad (39)$$

As follows from (37) and (38), the total power is always conserved as $\sum_{N=0}^\infty B_{00,N} = 0$.

Substituting all acceptance spectra into (32) one can find the entire matrix $\mathbf{\Lambda}$ that defines the average dynamics of the system. To validate the model, we calculated this matrix for the 120 lowest-order LG modes with $w = 40$ mm at a wavelength of $\lambda = 850$ nm and turbulent scales of $l_0 = 1.0$ mm, $L_0 = 1.0$ m, resulting in $\mathcal{I}_{00} = -5.57$. A relatively small L_0 was deliberately chosen to minimize the simulation errors associated with the numerical generation of phase screens by means of the Fourier method. We scaled the matrix to achieve the necessary interaction strengths $\Lambda_{00}L$ and calculated the matrix exponent (31) applied to the initial vector \mathbf{v}_0 with unit power in the fundamental mode and zero elsewhere.

As a reference, we used simulation results that were obtained by application of 10600 independent turbulence phase screens to the fundamental mode and calculating

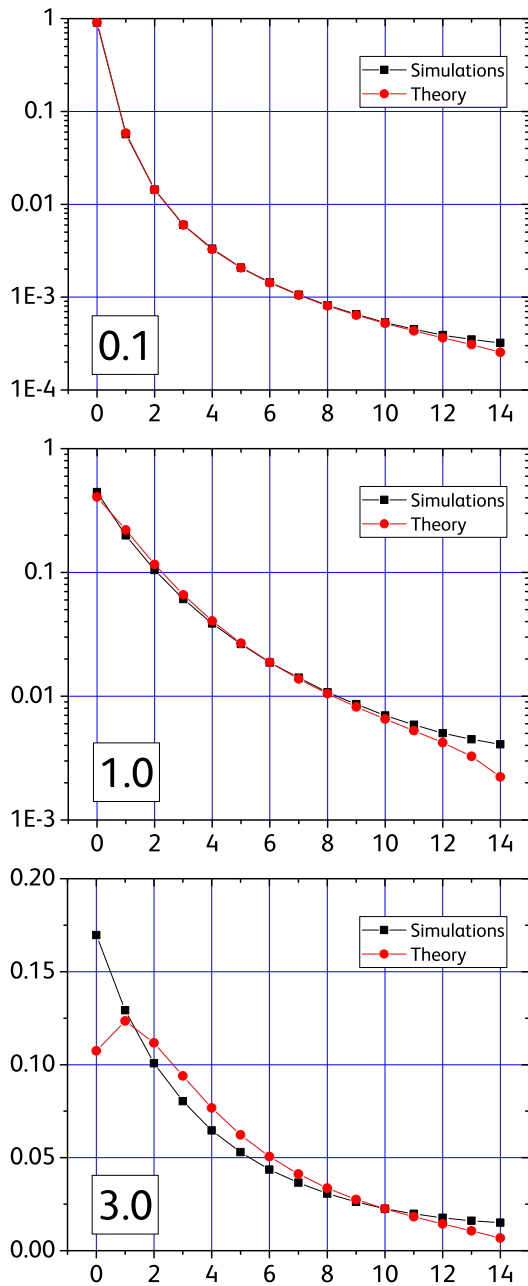


FIG. 2. Distribution of power among mode groups as a function of N for 3 channels with fundamental-mode input and characterized by interaction strengths $|\Lambda_{00}L| = 0.1, 1.0,$ and 3.0 , which is equivalent to Fried parameter values of 204 mm, 51.3 mm, and 26.6 mm respectively. Based on 120 lowest-order LG modes. The total power in these modes is 0.996, 0.95, and 0.8 respectively, while the rest is dissipated to even higher order modes.

the overlap with 120 lowest-order HG and LG modes. The strength of the turbulence was chosen by setting the Fried parameter r_0 to a value that produces the same $\Lambda_{00}L$ as in the model using (33). The turbulence scales l_0 and L_0 were the same as for the model. Phase screen gen-

eration is performed based on algorithm [16] with 828 frequency components for each axis, with the lowest spatial frequency (and the step between adjacent ones) of $f_0 = 0.2 \text{ m}^{-1}$. The simulation grid size is 1024×1024 points spaced at 0.267 mm.

To represent the distribution of power among modes in a concise way and to make the result independent of the choice of LG vs. HG, we calculated the total power for groups of modes with the same N . The results for the interaction strengths of 0.1, 1 and 3 are shown in Fig. 2. It must be noted that the simulation results based on the HG and LG mode families, after grouping by N , only differ by less than 2% relative error, which matches the expected averaging error.

As one can see at the interaction strength of 0.1 there is an excellent agreement with the simulation results with the only exception at the largest N , where the limited size of the matrix $\mathbf{\Lambda}$ does not take into account non-negligible scattering from modes with $N > 14$. At strength 1, the agreement becomes somewhat poorer, but still the model represents the simulation results with rather high precision. At the strength of 3 the dominating error is observed for the fundamental mode, where the model significantly underestimates its population. The main cause of this mismatch is the coherence between modes, which is discussed in detail in the next section.

V. APPLICABILITY OF THE MODEL AND DISCUSSION

A. Model applicability

The main simplification in our framework is neglecting the optical phases of the spatial modes. This does not affect the result if a single spatial mode is present in the channel. Therefore, if only a single mode is excited or if it strongly dominates over all other spatial modes, the analysis developed here is exact. However, if the original signal is a coherent superposition of two or more modes, the given description becomes inaccurate, as the two modes have certain phase relations and cannot be accurately described within the chosen optical field representation.

In fact, the amount of the transferred power is phase-dependent as the induced wave may interfere with the power already in the given spatial mode, either constructively or destructively. Therefore, the prediction for a coherent superposition is only fair for certain circumstances, where phase averaging does not become significantly biased due to the interference. If different spatial modes are mutually incoherent, our analysis is certainly applicable, as the two waves do not interfere.

This limitation also has consequences for the case of the Gaussian beam propagation studied. Although the initial beam comprises a single spatial mode, other spatial modes are generated due to the turbulent process. The amplitudes of such generation process may have a

dependence on the phase, which results in phase correlations between different modes. This breaks down assumptions and leads to prediction errors. Nevertheless, as one can see, the model still has a substantial predicting power even for quite strong turbulence levels.

Moreover, the original simulation did not include light propagation, i.e., technically, the phase screens had zero thickness. When propagation over distances comparable to z_R is taken into account, relative phases between modes with different N get smeared because of the propagation-dependent Gouy phase. This results in even better agreement with our model.

As an example, we simulated the same problem, but included propagation between $-z_R/2$ and $z_R/2$ relative to the beam waist position. The total distance of 5900 m was divided into 10 equal chunks with equal turbulence strengths in each. That makes the Rytov parameter for the interscreen distance about 0.05. It ensures a good precision of simulation because this value is below the widely-used margin of 0.1 [17]. Under these conditions, the radius w of the spatial modes varied by less than 12%, which was ignored in the theoretical model. Figure 3 shows the results.

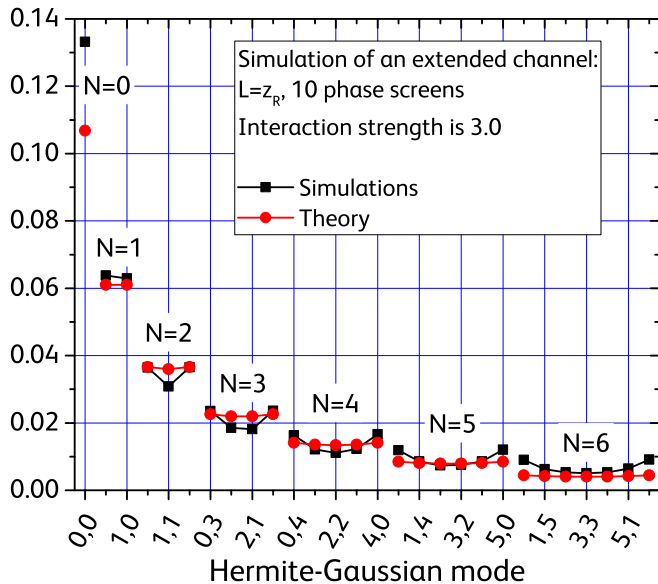


FIG. 3. Distribution of power among HG modes in an extended channel with the length of $L = 5900$ m and the interaction strength $|\Lambda_{00}L| = 3.0$. The Rytov parameter $\sigma_R^2 = 3.2$. Theoretical prediction, which does not depend on the channel length unless the beam diameter varies, is based on 28 lowest-order HG modes. Modes are presented in the following order: $(0,0)$, $(0,1)$, $(1,0)$, $(0,2)$, $(1,1)$, $(2,0)$, etc.

As one can see, in this extended channel the simulation result for the power in the fundamental mode $(0,133)$ is much closer to the theory prediction of 0.107 than the previous simulation with no propagation (0.170) . This is mainly due to the partial phase randomization between different modes due to beam propagation. In general,

there is strong agreement between our theoretical model and the simulation, with notable deviation for highest-order modes ($N = 6$). For them, the theory prediction is again noticeably lower due to the lack of power backflow from higher-order modes ignored while taking the matrix exponent.

To validate our simulation routine, we also simulated the same problem with 10 phase screens, but skipping beam propagation steps. The results perfectly matched the original single phase screen simulation up to the averaging error of less than a few percent.

B. Applicable turbulence strength

The strength of turbulence in a channel is typically defined by the Rytov parameter σ_R^2 . Comparing (9) with (32) we can express the Rytov parameter via the interaction strength $|\Lambda_{00}L|$:

$$\sigma_R^2 = 10.7 \frac{\Lambda_{00}L}{\mathcal{I}_{00}} \left(\frac{L}{kw^2} \right)^{5/6}. \quad (40)$$

In our simulation $|\mathcal{I}_{00}| = 5.57$, while it is upper-bounded by 11.9 (see the next subsection). If we assume that the diameter of the beam does not change significantly and $w(z) \approx w_0$, we can see that the ratio in parentheses is $L/(2z_R)$, which should not be larger than 1 to preserve the same diameter of the mode along the channel. Thus, in our example, the Rytov parameter is not larger than $1.9|\Lambda_{00}L|$. For the strongest interaction case studied of $|\Lambda_{00}L| = 3$, the Rytov parameter may be as large as 5.7. So we may say that our model is still reasonably applicable even for the medium-to-strong turbulence regime.

C. Convergence at $K \rightarrow 0$ and scalings for pure Kolmogorov turbulence

One major problem associated with a description of turbulent processes is the divergence of the Kolmogorov spectrum at $K \rightarrow 0$. Despite the available option of damping low-frequency components, we show that the developed framework is fully compatible with the undamped original spectrum (2). All acceptance spectra $B_{ab}(\vartheta)$ vanish at $\vartheta = 0$ and behave at most linearly at small arguments. This linear dependence only appears either for the same mode ($B_{aa} \approx -2[N+1]\vartheta$) or for the case when N changes by no more than 1. In all other cases, the acceptance spectrum scales as a higher power of ϑ . Thus, the integral (29) always converges at zero even for the Kolmogorov spectrum, in the worst case as $\int_0 \vartheta^{(-5/6)} d\vartheta$. Its convergence at infinity is also guaranteed by the exponential decay of the acceptance spectrum. Therefore, there is no technical limitation to applying our model to the unmodified Kolmogorov spectrum. Specifically, for

the power in the fundamental mode, we have

$$|\mathcal{I}_{00}^{\max}| = \int_0^\infty \vartheta^{-11/6} [1 - \exp(-2\vartheta)] d\vartheta \\ = \frac{6}{5} 2^{5/6} \Gamma(1/6) \approx 11.902, \quad (41)$$

which provides an upper bound for \mathcal{I}_{00} for any damped Kolmogorov spectrum. Despite that this is technically feasible, it may not have much practical importance as this marginal convergence at zero still results in a disproportionately large contribution from $K \rightarrow 0$.

Nevertheless, the research of the behavior of various modes in pure Kolmogorov turbulence draws enough attention [8–10]. This behavior can also be studied in the developed framework. We are going to specifically examine the diagonal elements of the propagation matrix Λ . As a recap, we emphasize that these diagonal elements are the exact relative rates of power loss from a given mode with propagation distance, provided it is the only mode excited in the channel. Thus, they indicate the strength of interaction between the mode in question and the turbulent medium. As we show below, they have a very prominent connection with the mode order N , a connection defined by the Kolmogorov spectral shape.

Among the different modes, the diagonal elements Λ_{aa} only differ by the value of the dimensionless integral \mathcal{I}_{aa} , which will be studied here. Both expressions for $B_{aa}(\vartheta)$ for the studied LG and HG mode families contain Laguerre polynomials. Thus, we can use the Mehler–Heine formula, which describes their scaling with increasing polynomial order:

$$\lim_{n \rightarrow \infty} L_n(x) = J_0(2\sqrt{nx}). \quad (42)$$

We start with the expression for LG modes, where we replace ϑ with x/N and p with βN :

$$\mathcal{I}_{pl;pl} = N^{5/6} \int_0^\infty x^{-11/6} \\ \times \left(1 - \left[L_{(1-\beta)N} \left(\frac{x}{N} \right) L_{\beta N} \left(\frac{x}{N} \right) \right]^2 \exp \left(-\frac{2x}{N} \right) \right) dx. \quad (43)$$

For increasing N the exponential term becomes unity, while Laguerre polynomials may be converted to Bessel functions. At this step, it becomes apparent that the dependence on N disappears within the integral. Moreover, since the $x^{-11/6}$ term gives a huge preference to small values of x , if we substitute $J_0(2t) \approx 1 - t^2$ we can see that the dependence on β also disappears. In reality, it exists, but is expected to be small.

Similar calculations for HG modes can be done with defining β as m/N . Have

$$\lim_{N \rightarrow \infty} \mathcal{I}_{mn;mn} = N^{5/6} \int_0^\infty x^{-11/6} \\ \times \left(1 - \left[J_0 \left(2 \cos \xi \sqrt{2\beta x} \right) J_0 \left(2 \sin \xi \sqrt{2(1-\beta)x} \right) \right]^2 \right) dx. \quad (44)$$

If, in addition, we use the approximation for small arguments of J_0 and perform averaging over ξ , we also see that the dependence on β disappears.

Therefore, for both mode families we see a clean asymptotics $\mathcal{I} \sim N^{5/6}$ with some minor dependence on the particular mode of order N . Explicit calculations for small mode orders reveal that the scaling is, in fact, $\mathcal{I} \approx 12(N+1)^{5/6}$, which is illustrated in Table I. It contains both the exact values of \mathcal{I} and this simplified scaling. As one can see, the relative error of such an approximation for the given set of modes is below 3% for HG modes and below 1% for LG modes!

Hence, we have shown that the strength of mode interaction with turbulent medium scales as $(N+1)^{5/6}$. Using (33) one can see that to achieve the same level of power dissipation $\Lambda_{aa}L$, the value of $(w/r_0)^{5/3}$ should be inversely proportional to \mathcal{I}_{aa} . That translates to $w\sqrt{N+1}/r_0 = \text{const.}$, which corresponds to a universal scaling law for the interaction strength with respect to the mode order. It becomes even more intuitive if one recalls that the intensity-weighted RMS radius of the beam for both HG and LG modes is $w\sqrt{(N+1)}/2$. So, the relative amount of power loss for different modes is only a function of the ratio of their RMS size and the Fried parameter.

The very same scaling for LG modes was previously empirically found in [9], and later confirmed in [10] and [8]. The authors of these works observe a universal dependence of some measurable quantity (like the concurrence or the ratio of the received power in modes with positive and negative values of l) for different modes, given that the Fried parameter is scaled by what they call the *phase correlation length* [10]. Indeed, these measurable parameters are directly tied to the strength of interaction with the turbulent medium, which scales with the mode order, as we have just demonstrated.

The only missing part in observing that the two scalings are indeed the same is a connection between the phase correlation length ξ and the mode order. Their definition of ξ for the mode LG_{pl} is $\xi = \sin[\pi/(2|l|)]\langle\rho\rangle$, where $\langle\rho\rangle$ is the intensity-weighted mean radius of the mode. This can be fairly accurately connected to the mentioned earlier RMS radius, because their largest mismatch is observed for the fundamental mode and is only around 13%, while it is significantly lower for modes with low values of p .

Papers [9, 10] only consider the case with $p = 0$, therefore $N = |l|$ and, thus, replacing sine function with its argument, we get the scaling $\xi \approx 1/\sqrt{N}$. It can be easily checked that for $|l| > 1$ this is a consistent approximation, which matches our results. In [8] authors also considered the case of non-zero p , however, as one can see from figure SF4, for $p = 5$, unlike the case $p = 0$, there is a significant separation between small and large values of $|l|$. This is because the real scaling of the interaction strength is given by the RMS mode size, while the phase correlation length was an empirical estimate that

N	0	1	2	2	3	3	4	4	4	5	5	5
LG		(0,-1)	(0,-2)		(0,-3)	(1,-1)	(0,-4)	(1,-2)		(0,-5)	(1,-3)	(2,-1)
modes	(0,0)	(0,1)	(0,2)	(1,0)	(0,3)	(1,1)	(0,4)	(1,2)	(2,0)	(0,5)	(1,3)	(2,1)
$\mathcal{I}_{pl;pl}$	11.902	21.406	30.088	29.961	38.281	38.130	46.130	45.981	45.892	53.716	53.577	53.450
HG		(0,1)	(0,2)		(0,3)	(1,2)	(0,4)	(1,3)		(0,5)	(1,4)	(2,3)
modes	(0,0)	(1,0)	(2,0)	(1,1)	(3,0)	(2,1)	(4,0)	(3,1)	(2,2)	(5,0)	(4,1)	(3,2)
$\mathcal{I}_{mn;mn}$	11.902	21.200	29.558	30.056	37.411	38.145	44.922	45.801	46.054	52.174	53.155	53.571
$12(N+1)^{5/6}$	12.000	21.382	29.977	29.977	38.098	38.098	45.883	45.883	45.883	53.412	53.412	53.412

TABLE I. Exact values of the dimensionless integral \mathcal{I}_{aa} for lowest order LG and HG modes and their approximation with a function of N . These values define the relative rates of power loss from a given mode with propagation distance for Kolmogorov turbulence.

becomes increasingly inaccurate for larger values of p .

D. Applications for adaptive pointing systems

Another observation, which may become very handy in practical applications, comes from the flexibility of our framework to accommodate arbitrary turbulence spectra. Most practical free-space optical links use some kind of a pointing, acquisition, and tracking (PAT) system. They significantly help in reduction of the channel loss in the presence of turbulence. A more advanced version of the PAT is some kind of adaptive optics for further correction of turbulent distortions.

All of these tools may be viewed as high-pass spatial filters for turbulent distortions, which effectively suppress phase fluctuations at low spatial frequencies, perceived in the first place as the angle of arrival fluctuations. Measuring the spectral response of these tools, one can find the effective residual phase fluctuations spectrum observed in the corrected optical channel. This residual spectrum can then be used within our framework to predict channel performance. Such an additional damping of the turbulence spectrum results in weaker interactions between spatial modes and, consequently, the improved overall performance.

E. Comparison with previous results

There are a very limited number of previous publications in which optical power in a particular spatial mode was studied. One notable example is [6], which analyzed the cross-talk for the pure phase vortex beams having uniform intensity within a circle. Although they are substantially different from the LG modes, the result for the power remaining in the same mode is $1 - 1.01(D/r_0)^{5/3}$ at the limit of $r_0 \rightarrow \infty$, where D is the diameter of the beam. Using (7) one can see that it indicates linear scaling with L , which exactly matches our findings for small perturbations. Similarly, the power in adjacent modes with a different OAM is shown to increase linearly, which also agrees with the present analysis. Unfortunately, the results for high levels of turbulence do not show a good

agreement both because our model becomes less accurate and because the pure vortex beams are not LG modes studied in our framework.

A similar picture appears when comparing with [5]. Its authors studied families of spatial modes carrying the same OAM. In fact, they analyzed a mode set, where the radial part is independent of the azimuthal mode order. This is not the case for LG modes, where the radial part depends on both the radial p and the azimuthal l parameters. Neither are they eigenfunctions of propagation, which is a critical requirement of our model. Thus, we can only confirm that the behavior under low turbulence levels shows a reasonably good agreement with this previous work. The matching is the best when more than 50% of the power remains with the particular OAM value. At even stronger turbulence levels, the two models become too different for a direct comparison.

A more accurate comparison can be made with the first-order approximation for the Gaussian beam from our previous work [19]. The strength of the turbulent action $|P_{00}|$, denoted $w^2 C_a/2$ in the cited work, is given by the same integral (28), but with the filtering function of $2\vartheta|F(K)|^2$ instead of $|B_{00}(\vartheta)| = 1 - \exp(-2\vartheta)$, where the low-pass filter $|F(K)|^2$ was introduced to account for the damping of high-frequency components due to spatial averaging. Both expressions exhibit exactly the same asymptotic behavior as $\vartheta \rightarrow 0$. The mean remaining power in the fundamental mode was $(1 + |P_{00}|)^{-1}$, whereas our present model, applied exclusively to the fundamental mode, yields $\exp(-|P_{00}|)$. The two expressions essentially coincide for small arguments and behave similarly for larger ones. Moreover, the same scaling (38) with N appears for scattering into higher-order modes. Overall, there is excellent agreement with this previous result in the low-frequency part of the spectrum and for not too strong turbulence, which is naturally expected given the limitations of the first-order approximation.

VI. CONCLUSION

In this paper, we presented a general approach describing spatial mode interactions induced by atmospheric turbulence in a free-space optical channel. We devel-

oped a straightforward framework and applied it to two common families of spatial modes: Hermite-Gaussian for Cartesian symmetry and Laguerre-Gaussian for cylindrical symmetry. The framework is based on the split-step propagation model, where we represent an optical field as a discrete distribution of optical power among a complete set of spatial modes. As this representation does not change with unperturbed propagation, the whole process effectively becomes an integral perturbation induced by infinitesimal phase screens.

One of the obtained fundamental results is that the mode interaction strength is proportional to the turbulent phase fluctuation power that overlaps with the spatial acceptance spectrum, specific for a given pair of interacting modes. Similarly, the optical power lost from a mode is also proportional to the total power of phase fluctuations within the specific spatial spectrum. Thus, as the power of phase fluctuations accumulates additively along the propagation, the induced interactions of the spatial modes are proportional to the propagation distance in uniform channels.

This result is exact for channels with a single excited spatial mode (or an incoherent combination of them) and weak turbulent perturbations. Taking into account a larger number of spatial modes for calculation of their dynamics, the same framework can be used to reliably predict the average distribution of optical power among spatial modes under medium-to-strong turbulence conditions. Comparison with full-scale simulations shows that the accuracy of our model improves with beam propagation for a given phase fluctuation power, as propaga-

tion smears phase relations between different modes. The matching would be ideal if the phases were randomized at each propagation step, which aligns with the assumption of full incoherence.

The developed framework helps to better understand the behavior of structured light in turbulent propagation conditions and it can also be used for quantitative estimations of modal cross-talk and the number of excited modes. The analytical expressions can also be used for validation and debugging of various simulation tools especially for unbounded spectra like Kolmogorov's, whose accurate accounting in simulations is non-trivial [14]. The developed tools were used to demonstrate the existence of a universal connection between the mode number and the rate of power dissipation, which was earlier found empirically for a subset of LG modes.

A particular advantage of the proposed model is its spectral-agnostic nature. It can be readily applied to the Kolmogorov spectrum and its derivatives, as well as to arbitrary spectra, which may appear in other types of stochastic propagation media. Similarly, it can model the behavior of a channel that is equipped with a precision optical tracking and adaptive optic systems. Those may be perceived as equivalent high-pass filters for the turbulent process, which effectively reduce the power of phase fluctuations and suppress modal cross-talk.

ACKNOWLEDGMENT

The author thanks James Grieve and Sana Amairi-Pyka for their support and assistance with the manuscript, and Stephen Vintskevich for stimulating discussions.

-
- [1] M. Mirhosseini, O. S. Magana-Loaiza, M. N. O'Sullivan, B. Rodenburg, M. Malik, M. P. J. Lavery, M. J. Padgett, D. J. Gauthier, and R. W. Boyd, High-dimensional quantum cryptography with twisted light, *New J. Phys.* **17**, 033033 (2015).
 - [2] A. Sit, F. Bouchard, R. Fickler, J. Gagnon-Bischoff, H. Larocque, K. Heshami, D. Elser, C. Peuntinger, K. Gunthner, B. Heim, C. Marquardt, G. Leuchs, R. W. Boyd, and E. Karimi, High-dimensional intracity quantum cryptography with structured photons, *Optica* **4**, 1006 (2017).
 - [3] D. Cozzolino, B. Da Lio, D. Bacco, and L. K. Oxenløwe, High-dimensional quantum communication: Benefits, progress, and future challenges, *Advanced Quantum Technologies* **2**, 1900038 (2019).
 - [4] D. A. B. Miller, Communicating with waves between volumes: evaluating orthogonal spatial channels and limits on coupling strengths, *Appl. Opt.* **39**, 1681 (2000).
 - [5] C. Paterson, Atmospheric turbulence and orbital angular momentum of single photons for optical communication, *Phys. Rev. Lett.* **94**, 153901 (2005).
 - [6] G. A. Tyler and R. W. Boyd, Influence of atmospheric turbulence on the propagation of quantum states of light carrying orbital angular momentum, *Opt. Lett.* **34**, 142 (2009).
 - [7] B. Rodenburg, M. P. J. Lavery, M. Malik, M. N. O'Sullivan, M. Mirhosseini, D. J. Robertson, M. Padgett, and R. W. Boyd, Influence of atmospheric turbulence on states of light carrying orbital angular momentum, *Opt. Lett.* **37**, 3735 (2012).
 - [8] D. Bachmann, A. Klug, M. Isoard, V. Shatokhin, G. Sorelli, A. Buchleitner, and A. Forbes, Universal crosstalk of twisted light in random media, *Phys. Rev. Lett.* **132**, 063801 (2024).
 - [9] A. Hamadou Ibrahim, F. S. Roux, M. McLaren, T. Konrad, and A. Forbes, Orbital-angular-momentum entanglement in turbulence, *Phys. Rev. A* **88**, 012312 (2013).
 - [10] N. D. Leonhard, V. N. Shatokhin, and A. Buchleitner, Universal entanglement decay of photonic-orbital-angular-momentum qubit states in atmospheric turbulence, *Phys. Rev. A* **91**, 012345 (2015).
 - [11] V. P. Aksenov, V. V. Kolosov, G. A. Filimonov, and C. E. Pogutsa, Orbital angular momentum of a laser beam in a turbulent medium: preservation of the average value and variance of fluctuations, *Journal of Optics* **18**, 054013 (2016).
 - [12] B. Ndagano, N. Mphuthi, G. Milione, and A. Forbes, Comparing mode-crosstalk and mode-dependent loss

- of laterally displaced orbital angular momentum and Hermite-Gaussian modes for free-space optical communication, *Opt. Lett.* **42**, 4175 (2017).
- [13] M. A. Cox, N. Mphuthi, I. Nape, N. Mashaba, L. Cheng, and A. Forbes, Structured light in turbulence, *IEEE J. Sel. Top. Quantum Electron.* **27**, 1 (2021).
- [14] C. Peters, V. Cocotos, and A. Forbes, Structured light in atmospheric turbulence—a guide to its digital implementation: tutorial, *Adv. Opt. Photon.* **17**, 113 (2025).
- [15] J. M. Martin and S. M. Flatté, Intensity images and statistics from numerical simulation of wave propagation in 3-d random media, *Appl. Opt.* **27**, 2111 (1988).
- [16] B. M. Welsh, Fourier-series-based atmospheric phase screen generator for simulating anisoplanatic geometries and temporal evolution, in *Propagation and Imaging through the Atmosphere*, Vol. 3125, edited by L. R. Bissonnette and C. Dainty, International Society for Optics and Photonics (SPIE, 1997) pp. 327 – 338.
- [17] M. Klen and A. A. Semenov, Numerical simulations of atmospheric quantum channels, *Phys. Rev. A* **108**, 033718 (2023).
- [18] D. Bachmann, M. Isoard, V. Shatokhin, G. Sorelli, and A. Buchleitner, Accurate zernike-corrected phase screens for arbitrary power spectra, *Opt. Engineering* **64**, 058102 (2025).
- [19] K. S. Kravtsov, A. K. Zhutov, I. V. Radchenko, and S. P. Kulik, Turbulence-induced optical loss and cross-talk in spatial-mode multiplexed or single-mode free-space communication channels, *Phys. Rev. A* **98**, 063831 (2018).
- [20] M. A. Cox, C. Rosales-Guzmán, M. P. J. Lavery, D. J. Versfeld, and A. Forbes, On the resilience of scalar and vector vortex modes in turbulence, *Opt. Express* **24**, 18105 (2016).
- [21] N. Mphuthi, R. Botha, and A. Forbes, Are Bessel beams resilient to aberrations and turbulence?, *J. Opt. Soc. Am. A* **35**, 1021 (2018).
- [22] R. R. Beland, Propagation through atmospheric optical turbulence, in *The Infrared & Electro-Optical Systems Handbook, Volume 2*, edited by F. G. Smith (SPIE Press / The Infrared Information Analysis Center, 1993) pp. 157–232, chapter 2.
- [23] R. Lawrence and J. Strohbehn, A survey of clear-air propagation effects relevant to optical communications, *Proceedings of the IEEE* **58**, 1523 (1970).
- [24] D. L. Fried, Optical resolution through a randomly inhomogeneous medium for very long and very short exposures, *J. Opt. Soc. Am.* **56**, 1372 (1966).
- [25] F. Roddier, V the effects of atmospheric turbulence in optical astronomy (Elsevier, 1981) pp. 281–376.
- [26] V. I. Tatarski, *The Effects of the Turbulent Atmosphere on Wave Propagation* (Israel Program for Scientific Translations., Jerusalem, Israel, 1971).
- [27] S. Danakas and P. K. Aravind, Analogies between 2 optical-systems (photon-beam splitters and laser-beams) and 2 quantum-systems (the 2-dimensional oscillator and the 2-dimensional hydrogen-atom), *Phys. Rev. A* **45**, 1973 (1992).
- [28] S. Restuccia, D. Giovannini, G. Gibson, and M. Padgett, Comparing the information capacity of Laguerre-Gaussian and Hermite-Gaussian modal sets in a finite-aperture system, *Opt. Express* **24**, 27127 (2016).
- [29] I. S. Gradshteyn and I. M. Ryzhik, *Table of Integrals, Series, and Products*, 7th ed., edited by A. Jeffrey and D. Zwillinger (Academic Press, Amsterdam, 2007).